



HAL
open science

Tool use and function knowledge shape visual object processing

Francois Foerster, Jeremy Goslin

► **To cite this version:**

Francois Foerster, Jeremy Goslin. Tool use and function knowledge shape visual object processing. *Biological Psychology*, 2021, 164, pp.108143. 10.1016/j.biopsycho.2021.108143 . hal-03419031

HAL Id: hal-03419031

<https://hal.science/hal-03419031>

Submitted on 2 Aug 2023

HAL is a multi-disciplinary open access archive for the deposit and dissemination of scientific research documents, whether they are published or not. The documents may come from teaching and research institutions in France or abroad, or from public or private research centers.

L'archive ouverte pluridisciplinaire **HAL**, est destinée au dépôt et à la diffusion de documents scientifiques de niveau recherche, publiés ou non, émanant des établissements d'enseignement et de recherche français ou étrangers, des laboratoires publics ou privés.



Distributed under a Creative Commons Attribution - NonCommercial 4.0 International License

1 Tool use and function knowledge shape visual object processing

2

3

Author names and affiliations

4

Francois Foerster ^A

5

^A University of Plymouth, School of Psychology, Drake Circus, Plymouth, Devon PL4 8AA, United Kingdom

6

francois.foerster@plymouth.ac.uk

7

8

Jeremy Goslin ^A

9

^A University of Plymouth, School of Psychology, Drake Circus, Plymouth, Devon PL4 8AA, United Kingdom

10

jeremy.goslin@plymouth.ac.uk

11

12

Corresponding author

13

Francois Foerster, PhD

14

University of Plymouth, School of Psychology, Drake Circus, Plymouth, Devon PL4 8AA, United Kingdom

15

francois.foerster@plymouth.ac.uk

16

17

18

Abstract

19 Perceiving the environment automatically informs how we can interact with it through
20 affordance mechanisms. However, it remains unknown how our knowledge about the
21 environment shapes how it is perceived. In this training study, we evaluated whether motor and
22 function knowledge about novel objects affects visual object processing. Forty-three participants
23 associated a usage or function to a novel object in interactive virtual reality while their EEG was
24 recorded. Both usage and function influenced the mu-band (8-12 Hz) rhythms, suggesting that
25 motor and function object information influence motor processing during object recognition.
26 Learning the usage also prevented the reduction of the theta-band (4–8 Hz) rhythms recorded
27 over the posterior cortical areas, suggesting a predominant top-down influence of tool use
28 information on visuo-motor pathways. The modulation being specifically induced by learning an
29 object usage, the results support further the embodied cognition approach rather than the
30 reasoning-based approach of object processing.

31

32 *Keywords:* EEG; affordance; object processing; embodied cognition; tool use

33

34

Introduction

35 The perceived world through our eyes appears automatically translated as potential
36 interaction with it (Gibson, 1979). This phenomenon called affordance rely on brain mechanisms
37 detecting and preparing possible actions through perception. Affordances can also be learned
38 through our everyday usage of objects and tools. In the last decade, affordance processing has
39 been highly investigated in cognitive neuroscience using neuroimaging techniques (de Wit, de
40 Vries, van der Kamp, & Withagen, 2017; Reynaud, Lesourd, Navarro, & Osiurak, 2016;

41 Sakreida et al., 2016; Thill, Caligiore, Borghi, Ziemke, & Baldassarre, 2013). fMRI analysis
42 unveiled the neuronal networks involved in the perception of and action triggered by the
43 affordances during object recognition (Brandi, Wohlschlager, Sorg, & Hermsdorfer, 2014;
44 Buxbaum, Kyle, Tang, & Detre, 2006; Mizelle, Kelly, & Wheaton, 2013; Sakreida et al., 2016;
45 Tettamanti, Conca, Falini, & Perani, 2017). Some networks being well-identified, understanding
46 their dynamics is the next milestone that cognitive and neuro-scientists have to reach (Kopell,
47 Gritton, Whittington, & Kramer, 2014). Our focus here is that affordance processing is never
48 naïve as perception is always relying on our pre-existing knowledge about the environment.
49 Consequently, how such top-down knowledge influences the automatic activation of visuomotor
50 pathways during object processing? To investigate this question, we used EEG recordings
51 coupled with an original virtual reality (VR) setup where participants perceived novel objects
52 trained beforehand with novel object knowledge, which is an object usage or a function. The
53 goal of the study was to test whether former object knowledge modulates the visual extraction of
54 affordances during object processing.

55 Recent theories suggest that alpha (8-12 Hz) and theta (4-8 Hz) rhythms control the
56 access to stored information in long-term memory via inhibition of task-irrelevant cell
57 assemblies in visual tasks (Jensen & Mazaheri, 2010; Klimesch, Fellinger, & Freunberger, 2011;
58 Klimesch, Freunberger, & Sauseng, 2010; Klimesch, Sauseng, & Hanslmayr, 2007). The
59 amplitude of occipital alpha oscillations and the synchronization of their phases are increased
60 during object recognition, reflecting the access and retrieval of semantic information
61 (Freunberger, Klimesch, Griesmayr, Sauseng, & Gruber, 2008). Also, the visual shape of objects
62 modulates the alpha oscillations recorded over posterior cortical areas during object recognition

63 (Vanni, Revonsuo, & Hari, 1997). Thus, alpha-band oscillations would signal the effect of top-
64 down object knowledge on affordance processing.

65 On a similar frequency-band but topographically and functionally distinct, mu-band
66 oscillations (8-12 Hz) are understood as a processing linking perception and action (Pineda,
67 2005). Recorded over central areas, they have been associated with motor planning (Llanos,
68 Rodriguez, Rodriguez-Sabate, Morales, & Sabate, 2013; Sabate, Llanos, Enriquez, & Rodriguez,
69 2012). Recently, Freeman et al. (2016) revealed that affording objects increases the central mu-
70 band power desynchronization during object processing. Similarly, Proverbio (2012) showed that
71 the perception of tools evokes less motor mu-band activity than non-tool objects, reflecting the
72 sensitivity of the mu-band in processing object affordance. Altogether, these studies revealed
73 markers of affordances processing. As an extension of these results, our training study
74 investigates the causal role played by usage and functional object knowledge on the dynamics of
75 visuo-motor processing of objects.

76 In this EEG study, we trained participants to manipulate two novel objects. Following the
77 appearance of an object and a tone, the task of the participant was to transport it from a location
78 to another. This motor task was chosen to guide the perception of the objects towards their
79 ecological value. In the middle of the experiment, half of the participants learned how to use one
80 of the two objects with a specific manipulation (usage condition). The other half of the
81 participants learned the function of one of the objects (function condition), without additional
82 manipulation. Following the additive model, one would expect that learning the object usage
83 would strengthen the activation of the motor system during object processing, as indexed by the
84 reduction of mu-band oscillatory activity (Freeman et al., 2016). However, previous work
85 indicated that the processing of visual and learned affordances interfere with each other due to

86 conflicting motor programs (Jax & Buxbaum, 2010; Kalénine, Wamain, Decroix, & Coello,
87 2016; Wamain, Sahai, Decroix, Coello, & Kalénine, 2018). Hence, an alternative hypothesis is
88 that learning an object usage reduces the activation of the motor system and be reflected as a
89 reduction of mu-band activity. Because the reduced activation would rely on motor conflicts,
90 such reduction would occur specifically when a manipulation is learned, and not following the
91 learning of the function.

92 The question is whether uniquely embodied motor information is involved in visual
93 object processing. Indeed, the alternative possibility is that objects and tools processing is
94 predominantly guided by semantic information, such as the object's function, as recently
95 suggested by the reasoning-based approach (Federico & Brandimonte, 2020; Osiurak & Badets,
96 2016; Osiurak, Rossetti, & Badets, 2017). Theoretically, we hypothesized that motor knowledge
97 induced by learning an object usage would interfere with the automatic extraction of visual
98 affordances. Practically, this would be expressed by increased reaction times (Jax & Buxbaum,
99 2010), and reduced early alpha-band synchronization (Wamain et al., 2018) and late motor mu-
100 band desynchronization (Freeman et al., 2016) recorded over centro-parietal cortical areas.
101 Training participants to learn an object function without a manipulation offered a control
102 condition to test the specific impact of motor knowledge on visual object processing. These
103 hypotheses were investigated on both phases and amplitudes of occipital alpha and motor mu-
104 band (8-12 Hz) oscillations.

105 **Methods**

106 **Participants**

107 Forty-three adult volunteers (mean age = 21 years old, range 19-29, including 12 males)
108 from the University of Plymouth participated in the study in exchange for money or course

109 credit. All participants reported being right-handed and having normal vision. Due to the use of a
110 VR headset, participants wearing correction glasses were not accepted. EEG data from six
111 participants were removed due to excessive numbers of artifacts. The experimental procedure
112 and written consent form for this study were approved by the ethics committee of the University
113 of Plymouth and conform with the 2008 Helsinki Declaration.

114 **Experimental setup and procedure**

115 The experiment used Unity software (Unity technologies, version 7.1.0f3) to create the
116 virtual environment and the HTC Vive (HTC Corp.) headset and controllers. Participants were
117 wearing both the EEG and VR headsets and were seated in a chair next to a desk. A button box
118 was placed on the desk situated on the right side of the participants and connected to the
119 computer to detect movement onsets. The virtual environment was composed of a small wooden
120 textured box, a white and a red dashed area situated on the table, a big box situated in front of the
121 participant and, a small black cube on their left (Fig. 1A). The size and height of the room,
122 virtual table, and the button box were fitted to the dimensions of the physical environment. For a
123 comfortable position of the hand on the button box, the distance between the chair and the desk
124 was adjusted for each participant. Participants were instructed to manipulate a VR controller,
125 represented by two possible 3-D models (Fig. 1B).

126 The experiment was divided into three phases termed as pre-training, training, and post-
127 training phases composed of 120 trials, 50 trials, and 120 trials, respectively. The trials for the
128 pre-training and post-training phases were divided into four blocks of 30 trials. The training
129 phase was divided into two blocks of 25 trials. After each block of trials, a time break was
130 proposed to the participant and the VR headset was removed if desired. The pre-training period
131 was used to control the possible effects of visual attention and familiarity with the two stimuli

132 and the task on the EEG activities. The trial procedure is depicted in Fig. 1C. At the beginning of
133 each trial, the participant had to place the right hand on the button box and look at the white
134 fixation cross situated in the front of him/her, at the location of the invisible controller. After
135 1000 ms, the fixation cross disappeared. Subsequently, one of two visual representations of the
136 controller appeared after a random time interval between 1000 ms and 1400 ms. Participants
137 were instructed to prepare to grasp-and-move the controller from the white to the red area after
138 hearing a tone (i.e. go-signal) triggered after a random time interval between 800 ms and 1200
139 ms. We used this delayed response paradigm to prevent contamination of the EEG signal from
140 movement-related effects. Once the controller was placed on the red area, next to the black cube,
141 the participant was instructed to return it to the white area. Then, the 3-D model of the controller
142 disappeared. The black cube had no other importance in the experiment. The motor task had to
143 be performed as fast as possible. If the button box was released before the onset of the go-signal,
144 the participant received a written feedback on a virtual panel at the end of the trial, reminding
145 him/her to move only after the tone. At the end of each trial, participants were instructed to put
146 their right hand back on the button when ready to start a new trial. Participants were instructed to
147 avoid movements and eye blinks during the trials, especially before the go-signal. They were
148 able to move freely between trials. The visual representation of the controller was randomly
149 assigned to each trial.

150 During both pre-training and post-training phases, participants had to grasp-and-move the
151 two object-stimuli without distinction. The purpose of the training phase was to transform the
152 representation of one of the two objects into a tool (i.e. a key that opens the box on the table).
153 The object trained was randomly assigned to each participant at the beginning of the training

154 phase. Following a mixed experimental design, two different trainings (usage vs function
155 conditions) represented a between-subject factor.

156 **Training phase in the function condition**

157 In the training phase of the function condition, 22 participants were instructed to grasp-
158 and-move both objects. When transported on the red area, the trained object triggered an audio-
159 visual animation of the opening of a box located in the front of the participant. The transportation
160 of the non-trained object did not trigger any sound or animation. Hence, in the function
161 condition, participants associated with the trained object the novel function information “a key
162 that opens the box”, as mentioned by the experimenter. Crucially, no additional motor
163 information was learned.

164 **Training phase in the usage condition**

165 In the usage condition, 21 participants were trained to execute a challenging key-like
166 movement with the trained object. At the commencement of the training, a very brief video was
167 depicting the usage of the object to learn and perform. The participants were instructed to
168 perform the tool use when the trained object appeared and the grasp-to-move action when the
169 non-trained object appeared. The tool use learned by the participants was a series of three
170 rotations (i.e. to the left, to the right, and to the left again) of the object in the hole of the wooden
171 box to open it. The rotations were restricted by the respective angles: turn the controller 90° to
172 the left, then turn 180° to the right, and finally turn 90° to the left back to the center, with a
173 precision of $\pm 10^\circ$. Exceeding $\pm 10^\circ$ of precision failed to open the box and consequently of the
174 trial. After the three rotations, the trigger button of the controller must have been pressed to open
175 the box, thus constraining the handgrip associated with the tool use. At the end of a failed trial,
176 participants received feedback advising which rotation was performed incorrectly, assuring

177 motor learning. Following a correct series of rotations and button press, the same audio-visual
178 animation as in the training of the object function was triggered. Thus, in the usage condition,
179 participants associated both novel function information "a key that opens the box", as mentioned
180 by the experimenter, and novel motor information (i.e. a handgrip, wrists rotations and a button
181 press).

182 **Behavioral and electroencephalographic recording**

183 The release of the button box was used to calculate the movement onset of the
184 participant. Then, the lift of the grasped controller was detected and used to calculate the
185 grasping onset. The action onset was detected when the objects were transported to the red area.
186 The object and movement onsets were used to time-lock EEG analysis. The action sequence was
187 segmented and calculated as follow: a) Initiation times, as the time between go-signal onsets and
188 movement onsets; b) Grasping times, as the time between movement onsets and grasping onsets;
189 c) Execution times, as the time between grasping onsets and action onsets. We evaluated these
190 time intervals depending on the stimulus-object during the and pre- and post-training phases of
191 each condition. EEG data were collected from 61 actively amplified Ag/AgCl electrodes
192 (easyCAP, Brain Products, Gilching, Germany) mounted on an elastic cap and following the
193 standard International 10-20 montage. Electrode impedances were kept below 20 k Ω . The
194 signals were amplified using a BrainAmp MR Plus amplifier (Brain Products) and continuously
195 sampled at 500 Hz. The virtual environment and the EEG recording were run on separate
196 computers.

197 **Data processing**

198 The training paradigm implemented in this experiment was chosen to estimate the
199 Training Effect (TE) of a given object, reflecting the specific consequences of learning the

200 function and usage of the objects on reaction times and EEG activities. This TE was calculated
201 with the following formula: $TE = \text{object}_{\text{post-training}} - \text{object}_{\text{pre-training}}$. This TE was calculated
202 separately for the trained and non-trained objects in both conditions (learning usage or learning
203 function). Hence, the comparison of the TE for the trained and non-trained objects allowed to
204 isolate the effect of the training. Therefore, it is hypothesized that the TE values concerning the
205 non-trained object would be minimal whereas the TE values about the trained object would be
206 maximal.

207 Only successful trials during the pre- and post-training phases were used for the
208 behavioral and EEG analyses. Successful trials were defined as trials where participants initiated
209 the action after the go-signal onset.

210 EEG recordings were processed with MNE-Python (Gramfort et al., 2014, 2013). Data
211 were filtered with a .1 Hz high pass filter and a 40 Hz low pass filter. The friction of the VR
212 headset on the frontal and prefrontal electrodes (Fp1, Fp2, F7, F3, Fz, F4, F8, Fpz, AF7, AF3,
213 AF4, AF8, F5, F1, F2, F6) during testing motivated us to remove these channels during data
214 cleaning to increase the signal-noise ratio. Each trial was time-locked on the object onset and
215 included a length of 2400ms, starting 1200ms before the object onset and finishing 1200ms after
216 the object onset. The Autoreject algorithm (Jas, Engemann, Bekhti, Raimondo, & Gramfort,
217 2017) was used to detect and repair artifacts. The motivation to use this algorithm was to
218 maximize the signal-noise ratio in adapting automatically the artefact detection parameters for
219 each participant. It implements topographic interpolations (Perrin, Pernier, Bertrand, & Echallier,
220 1989) to correct bad segments. The signal of each trial was then transformed using a surface
221 Laplacian filter, resulting in a reference-free current source density (CSD) which increases the

222 spatial resolution of the signal and reduces the artifacts due to volume conduction (Kayser &
223 Tenke, 2015b, 2015a; Tenke & Kayser, 2012).

224 Time-frequency representations (TFRs) of the oscillatory activity were computed for
225 each trial using a wavelet approach (Tallon-Baudry & Bertrand, 1999) to evaluate the specificity
226 of the TE on the alpha and mu-band oscillations. A family of Morlet wavelets (Gaussian-
227 windowed complex sine wave) was built to perform the convolution via fast Fourier transform
228 over each channel. The family of wavelets was parametrized to extract frequencies from 4 Hz to
229 35 Hz. The number of cycles of the wavelets was linearly-adapted, from 3 cycles for the lowest
230 frequency and 10 cycles for the highest frequency. This precaution was used to keep a well-
231 balanced trade-off between time and frequency resolution at each frequency. Following the
232 convolution, each trial vector was re-segmented on a time-window starting 1000 ms before the
233 object onset and finishing 800 ms after the object onset. This re-segmentation allowed the
234 removal of edge artifacts.

235 On one hand, to evaluate the TE on the amplitude of the mu-band oscillations, the CSD
236 signals were transformed into decibels relative to a baseline, where the baseline represents the
237 averaged signal from -1000 to 0 ms period relative to the object onset.

238 On the other hand, to evaluate the TE on the phase of the mu-band oscillations, the inter-
239 trial coherence (ITC, also called inter-trial phase-coherence, phase-locking factor, or phase-
240 locking value Lachaux et al., 1999) was calculated. The ITC corresponds to the magnitude of the
241 amplitude-normalized complex numbers averaged across trials for each time point, frequency,
242 condition, and electrodes of interest. Ranging from 0 to 1, a value of 0 representing an absence of
243 synchronization of phases across trials, and a value of 1 representing a perfect synchronization of
244 the phases over trials. Hence, the ITC coupled with amplitude analysis helped to disentangle

245 evoked from induced oscillatory activities. For each participant, the calculation of the ITC
246 involved an equal total number of trials within each condition.

247 **Statistical Analysis**

248 RStudio (v. 0.99.489) and the rstatix (v. 0.6.0) package were used to perform analysis of
249 variances (ANOVAs) and planned comparisons analysis with Tukey's HSD tests.

250 Concerning the behavioral data, repeated-measures mixed-design ANOVAs were
251 performed, with the Stimulus (trained vs non-trained object) as a within-subjects independent
252 variable and the Training (usage vs function conditions) as a between-subjects independent
253 variable. The TE on Movement, Grasping and Action Times were entered as dependent
254 variables.

255 Concerning the EEG data, the activation of the visual system has been evaluated through
256 the analysis of the alpha-band (8-12 Hz) activity recorded over the midline occipital electrode Oz
257 and the activation of the motor system through the analysis of the mu-band (8-12 Hz) activity
258 recorded over the midline centro-parietal electrode CPz (as in Proverbio, 2012; Wamain,
259 Gabrielli, & Coello, 2016; Wamain et al., 2018). These two electrodes were selected to test our
260 hypothesis. However, electrodes C3 and C4, located over left and right motor areas, respectively,
261 have also been found sensitive to the motor activation indexed by the mu-band oscillations
262 (Cannon et al., 2014; Muthukumaraswamy, Johnson, & McNair, 2004). Hence, electrodes C3
263 and C4 were also analyzed to evaluate the broad/narrow activation of the motor network during
264 visual object processing. Electrodes CPz, Oz, C3 and C4 represented the four regions of interest
265 (ROIs). The EEG signals of interest were the 8–12 Hz log-transformed (decibels) amplitude and
266 ITC. Oscillatory amplitudes were converted into decibels to facilitate statistical comparisons and
267 interpretation. Given that 1) the possible alpha modulation would occur following a minimum of

268 one cycle (i.e. 100 ms for an oscillation of 10 Hz), 2) last a few cycles, and 3) could be
269 contaminated from a potential tone onset, the time window of interest concerned the 100–600 ms
270 time interval following the object onset. To calculate the TE on the EEG data, the 8–12 Hz
271 amplitude and ITC recorded within the 100–600 ms time interval following the object onset were
272 averaged for each ROI. Repeated-measures mixed-design ANOVAs were performed, with the
273 Stimulus (trained vs non-trained object) and the ROI (CPz, Oz, C3 and C4) as within-subjects
274 independent variables and the Training (usage vs function conditions) as a between-subjects
275 independent variable. The TE on the mu-band amplitude and ITC were entered as dependent
276 variables.

277 **Data availability statement.**

278 A public data repository containing scripts and data is available at <https://osf.io/6bjuz/>.

279

Results

280 **Behavioral Results**

281 First, movement times below 200 ms were considered as errors (i.e. default in the button
282 press) and were discarded, representing 3.99 % of the trials. Second, for each participant and
283 each movement, grasping and action times above or below four standard deviations from the
284 mean were considered as outliers and removed, representing 4.92 % of the remaining trials.

285 During the training phase in usage condition, participants correctly performed the
286 challenging tool use in 40.2% and 52.5% of the trials in the first and second trial blocks,
287 respectively. A Pearson correlation analysis between the trial number and the percentage of
288 success to perform the tool use in the training phase indicated a reliable increase of the
289 performance over time ($r = .50, p < .0001$). The ANOVA evaluating the TE on Movement Times
290 did not revealed effects of the Stimulus ($F(1,47) < 0.01; p = .99, \eta^2_p < .001$), the Training ($F(1,$
291 $47) = 0.24; p = .63, \eta^2_p < .001$) nor their interaction ($F(1, 47) = 1.69; p = .20, \eta^2_p < .001$).

292 Concerning the TE on Grasping Times, the ANOVA did not indicated effects of the Stimulus
293 ($F(1, 47) = 0.08$; $p = .78$, $\eta^2_p < .001$), the Training ($F(1, 47) = 2.36$; $p = .13$, $\eta^2_p = .047$) nor their
294 interaction ($F(1, 47) = .35$; $p = .55$, $\eta^2_p < .001$). Similarly, the ANOVA evaluating the TE on
295 Action Times did not revealed effects of the Stimulus ($F(1,47) = 0.45$; $p = .50$, $\eta^2_p = .001$), the
296 Training ($F(1, 47) = 0.02$; $p = .89$, $\eta^2_p = .001$) nor their interaction ($F(1, 47) = 0.76$; $p = .39$, $\eta^2_p =$
297 $.002$).

298 **Electrophysiological Results**

299 The EEG analysis revealed a clear increase of amplitude in the theta-band (4-8 Hz) in the
300 first 400 ms following the onset of all objects (Fig. 2). Then, the alpha- and beta-band (16-24 Hz)
301 signal amplitude reduced in 200-800 ms time-window, as found in (Kourtis & Vingerhoets,
302 2015).

303 The ANOVA on the 8-12 Hz signal amplitude revealed a main effect of the Stimulus
304 ($F(1,156) = 7.29$, $p = .008$, $\eta^2_p = .024$), such as the TE were increased for non-trained objects
305 (Mean = -0.11 dB, CI = 0.04 dB) compared with the trained objects (Mean = -0.03 dB, CI = 0.04
306 dB, Fig. 3). This TE reflects a reduction of the mu-band amplitude specific to non-trained
307 objects, independently of the type of training. This also means that the trainings prevented the
308 reduction of the mu-band amplitude during visual processing of the trained objects. No other
309 main (all $F < 0.52$; all $p > .47$, all $\eta^2_p < .002$) or interaction effects were reported (all $F < 0.3$; all
310 $p > .65$, all $\eta^2_p < .003$).

311 The ITC analysis indicated a strong synchronization in the first 200 ms following object
312 perception, especially in the 4-10 Hz frequency range. The ANOVA revealed an effect of the
313 Training ($F(1,156) = 4.89$, $p = .028$, $\eta^2_p = .018$), with the TE on the 8-12 Hz ITC being generally
314 reduced across the four ROIs when learning the object function (Mean = -0.01, CI = 0.01)

315 compared with the learning the object usage (Mean = -0.03, CI = 0.01). The ANOVA also
316 revealed a marginally significant interaction effect between the Training and the Stimulus
317 ($F(1,156) = 3.89, p = .051, \eta^2_p = .011$). The TE on the ITC seemed reduced for the trained object
318 (Mean = -0.03, CI = 0.02) compared with the non-trained object (Mean = -0.01, CI = 0.02) when
319 learning the function ($p = .059$) but not in learning the usage ($p = .566$). The ANOVA did not
320 reveal other effect (all $F < 1.54$; all $p > .22$, all $\eta^2_p < .008$) on the TE of the 8-12 Hz ITC.

321 The visualization of the TFRs of the TE on the ITC did not reveal particular modulation
322 across the frequency spectrum. However, the TFRs show that the apparent 8-12 Hz oscillatory
323 signal originates from slower theta-band activity. The visualization of the TFRs of the TE
324 showed that the amplitude of slow oscillations was frequency-specific and very distinct in the
325 two learning conditions (Fig. 2). A post-hoc ANOVA has been conducted to test the TE on the
326 theta-band (4-8 Hz) amplitude depending on the Stimulus, Training and ROIs. The analysis
327 revealed a main effect of the Stimulus ($F(1,156) = 15.68, p = .0001, \eta^2_p = .038$), such as the TE
328 was increased for non-trained objects (Mean = -0.14 dB, CI = 0.04 dB) compared with the
329 trained objects (Mean = -0.05 dB, CI = 0.04 dB, Fig. 4). Crucially, the analysis indicated a
330 significant interaction effect between the Stimulus and the Training ($F(1,117) = 6.12, p = .014,$
331 $\eta^2_p = .015$), with the TE on the amplitude of theta-band oscillations being significantly reduced
332 for the non-trained object (Mean = -0.19 dB, CI = 0.06 dB) compared with the trained object
333 (Mean = -0.04 dB, CI = 0.05 dB) when learning the usage ($p < .0001$) but not when learning the
334 function only ($p = .34$). This indicates a modulation of theta-band oscillations during visual
335 object processing, but specifically when the object is associated with motor content. The
336 ANOVA did not reveal any other effect (all $F < 1.51$; all $p > .22$, all $\eta^2_p < .006$).

337

Discussion

338 In this study, we assessed whether the affordance processing of objects is primarily
339 guided by motor and/or semantic information, hence defending either the embodied cognition or
340 reasoning-based approach of visual object processing. Using an immersive virtual reality setup
341 coupled with EEG recording, participants were trained with novel object usage or function
342 before and after performing a delayed grasp-and-move task. In both training conditions, the EEG
343 training effects were particularly visible on the non-trained objects. This means that the
344 processing of the non-trained objects, rather than the trained objects, differed in the pre- and
345 post-training phases. Therefore, these effects suggest that training the objects prevented the
346 reduction of the EEG signals during visual object processing that would have occurred
347 otherwise. In this sense, both functional and motoric information modulated the motor network
348 during visual object processing, as indexed by the mu-band oscillations. However, only the
349 learning of tool use increased the posterior theta-band activity. This brings novel information on
350 the mechanistic role played by theta-band rhythms and learned object information on perception,
351 such as visual object processing appears predominantly guided by embodied motor knowledge
352 rather than conceptual knowledge about the function.

353 We expected delays in reaction times with the trained compared to the non-trained object
354 induced via the tool use training, indicating a competition between the multiple action
355 components recruited during recognition (Cisek, 2007; Cisek & Kalaska, 2005, 2010), such as
356 different handgrips, as found in previous studies (Jax & Buxbaum, 2010, 2013). Indeed,
357 participants reported using a different hand grip to perform the tool use during the training phase.
358 However, the analysis of the behavioral TE effect did not reveal such lags. The most likely
359 reason is that, in our delayed-response paradigm, the pre-tone periods were long enough to plan

360 robust motor decisions. Considering only our behavioral data, the study would support the
361 literature proposing that motor knowledge about objects is selectively activated upon task
362 requirements (Daprati & Sirigu, 2006; Lindemann, Stenneken, van Schie, & Bekkering, 2006).
363 However, our EEG data surely challenge this claim.

364 In both learning conditions, the trained objects were associated with the perceptual
365 outcome of the box opening. Thus, the theta-band modulations induced by learning the object
366 usage might rely primarily on the manipulative information rather than the visual information
367 associated with the novel object. This would indicate that, along with the motor mu-band
368 oscillation, the increase of the posterior theta-band oscillatory activity directly depends on the
369 learned object affordance (Borghi & Riggio, 2015). The present EEG analysis revealed evidence
370 that associating function knowledge to a novel object suffices to shape motor processing
371 involved during object recognition. Associating motor contents along with such function
372 knowledge (i.e. the tool use) impacted the theta-band activity recorded in a broad range of
373 posterior cortical areas during object recognition.

374 Theta rhythms have been associated with executive control (Cavanagh & Frank, 2014;
375 Harper, Malone, & Bernat, 2014; Töllner et al., 2017), attention mechanisms (Clayton, Yeung, &
376 Kadosh, 2015) and working memory (Gulbinaite, van Rijn, & Cohen, 2014; Klimesch et al.,
377 2010). Theta rhythms play a role in large-scale network communication allowing the access to
378 episodic and recent information from memory (see Herweg, Solomon, & Kahana, 2020;
379 Klimesch et al., 2010 for reviews), crucial for object recognition. Using an incidental learning
380 task, Hanslmayr, Spitzer, & Bäuml (2009) found that parietal theta-band event-related
381 synchronization (ERS) is associated with the recollection of non-semantic information. The
382 present training effect on theta-band activity could reflect the influence of top-down information

383 derived from memory on the bilateral Structure system, that is the dorso-dorsal visuo-motor
384 pathways specialized in the extraction of the geometrical features crucial for grasping actions.
385 The results suggest that novel embodied motor representations contribute to the activation of the
386 Structure system during object recognition. This contribution would occur even when the
387 perception is influenced by tool use representations irrelevant to the task at hand, such as
388 grasping to move the object. It would support the affordance competition hypothesis (Cisek,
389 2007; Cisek & Kalaska, 2010) proposing that all motor representations, even irrelevant ones to
390 the task, are gathered to feed action decision-making processing. Hence, one could question the
391 behavioral relevance to distinguish task-relevant from task-irrelevant motor representations
392 involved in perceptual processing such as object recognition.

393 A recent eye-tracking study suggested that object and tool recognition relies on the visual
394 decoding of the functional ends (Federico & Brandimonte, 2020), indicating that semantic
395 information, rather than motor information, is at the core of the processing. Theoretically, such a
396 proposal question whether tools are primarily grounded on sensorimotor (embodied cognition
397 approach) or semantic (reasoning-based approach) representations. Experimentally, the problem
398 with known tools is that they are always associated with both sensorimotor and semantic
399 knowledge and can be hardly isolated. The present EEG results suggest that semantics can affect
400 motor processing during object recognition. However, tool use information remained the
401 predominant source of top-down modulation on distributed visuo-motor pathways, hence
402 favoring the embodied approach of object processing. Supporting this idea, a recent study
403 showed that learning semantic invariants such as an object label influences object processing and
404 the oscillatory activity in posterior cortical areas, but only when a novel manipulation (i.e. a tool
405 use) is learned simultaneously (Foerster, Borghi, & Goslin, 2020).

406 In conclusion, tool use information, rather than function information, represent the main
407 source of influence on visual object processing. This effect relies on theta-band oscillation,
408 which could sign for the activation of learned affordances in action systems (Borghi & Riggio,
409 2015). Learning a novel tool use or a tool function affected the mu-band oscillations, which
410 suggests that both motor and function knowledge about the surrounding objects interfere with the
411 processing of their visual affordance.

412 Acknowledgments

413 This work was supported by the European Union's Horizon 2020 research and innovation
414 programme under the Marie Skłodowska-Curie grant agreement [642667].

415 Reference

- 416 Borghi, A. M., & Riggio, L. (2015). Stable and variable affordances are both automatic and
417 flexible. *Frontiers in Human Neuroscience*, 9(June), 351.
418 <https://doi.org/10.3389/fnhum.2015.00351>
- 419 Brandi, M.-L., Wohlschläger, A., Sorg, C., & Hermsdorfer, J. (2014). The Neural Correlates of
420 Planning and Executing Actual Tool Use. *Journal of Neuroscience*, 34(39), 13183–13194.
421 <https://doi.org/10.1523/JNEUROSCI.0597-14.2014>
- 422 Buxbaum, L. J., Kyle, K. M., Tang, K., & Detre, J. A. (2006). Neural substrates of knowledge of
423 hand postures for object grasping and functional object use: Evidence from fMRI. *Brain
424 Research*, 1117(1), 175–185. <https://doi.org/10.1016/j.brainres.2006.08.010>
- 425 Cannon, E. N., Yoo, K. H., Vanderwert, R. E., Ferrari, P. F., Woodward, A. L., & Fox, N. A.
426 (2014). Action experience, more than observation, influences mu rhythm
427 desynchronization. *PLoS ONE*, 9(3), 1–8. <https://doi.org/10.1371/journal.pone.0092002>
- 428 Cavanagh, J. F., & Frank, M. J. (2014). Frontal theta as a mechanism for cognitive control.

429 *Trends in Cognitive Sciences*, 18(8), 414–421. <https://doi.org/10.1016/j.tics.2014.04.012>

430 Cisek, P. (2007). Cortical mechanisms of action selection: the affordance competition
431 hypothesis. *Philosophical Transactions of the Royal Society of London. Series B, Biological*
432 *Sciences*, 362(1485), 1585–1599. <https://doi.org/10.1098/rstb.2007.2054>

433 Cisek, P., & Kalaska, J. F. (2005). Neural correlates of reaching decisions in dorsal premotor
434 cortex: Specification of multiple direction choices and final selection of action. *Neuron*,
435 45(5), 801–814. <https://doi.org/10.1016/j.neuron.2005.01.027>

436 Cisek, P., & Kalaska, J. F. (2010). Neural Mechanisms for Interacting with a World Full of
437 Action Choices. *Annual Review of Neuroscience*, 33(March), 269–298.
438 <https://doi.org/10.1146/annurev.neuro.051508.135409>

439 Clayton, M. S., Yeung, N., & Kadosh, R. C. (2015). The roles of cortical oscillations in sustained
440 attention. *Trends in Cognitive Sciences*, 19(4), 188–195.
441 <https://doi.org/10.1016/j.tics.2015.02.004>

442 Daprati, E., & Sirigu, A. (2006). How we interact with objects: learning from brain lesions.
443 *Trends in Cognitive Sciences*, 10(6), 265–270. <https://doi.org/10.1016/j.tics.2006.04.005>

444 de Wit, M. M., de Vries, S., van der Kamp, J., & Withagen, R. (2017). Affordances and
445 neuroscience: Steps towards a successful marriage. *Neuroscience and Biobehavioral*
446 *Reviews*, 80(February), 622–629. <https://doi.org/10.1016/j.neubiorev.2017.07.008>

447 Federico, G., & Brandimonte, M. A. (2020). Looking to recognise: the pre-eminence of semantic
448 over sensorimotor processing in human tool use. *Scientific Reports*, 10(1), 6157.
449 <https://doi.org/10.1038/s41598-020-63045-0>

450 Foerster, F. R., Borghi, A. M., & Goslin, J. (2020). Labels strengthen motor learning of new
451 tools. *Cortex*, 129, 1–10. <https://doi.org/10.1016/j.cortex.2020.04.006>

452 Freeman, S. M., Itthipuripat, S., & Aron, A. R. (2016). High working memory load increases
453 intracortical inhibition in primary motor cortex and diminishes the motor affordance effect.
454 *Journal of Neuroscience*, 36(20), 5544–5555. [https://doi.org/10.1523/JNEUROSCI.0284-](https://doi.org/10.1523/JNEUROSCI.0284-16.2016)
455 16.2016

456 Freunberger, R., Klimesch, W., Griesmayr, B., Sauseng, P., & Gruber, W. (2008). Alpha phase
457 coupling reflects object recognition. *NeuroImage*, 42(2), 928–935.
458 <https://doi.org/10.1016/j.neuroimage.2008.05.020>

459 Gibson, J. J. (1979). *The Ecological Approach to Visual Perception: Classic Edition*. (Boston:
460 Houghton Mifflin, Ed.). <https://doi.org/10.1002/bs.3830260313>

461 Gramfort, A., Luessi, M., Larson, E., Engemann, D. A., Strohmeier, D., Brodbeck, C., ...
462 Hämäläinen, M. S. (2014). MNE software for processing MEG and EEG data. *NeuroImage*,
463 86, 446–460. <https://doi.org/10.1016/j.neuroimage.2013.10.027>

464 Gramfort, A., Luessi, M., Larson, E., Engemann, D. A., Strohmeier, D., Christian, B., ...
465 Hämäläinen, M. (2013). MEG and EEG data analysis with MNE-Python. *Frontiers in*
466 *Neuroscience*, 7(December), 1–13. <https://doi.org/10.3389/fnins.2013.00267>

467 Gulbinaite, R., van Rijn, H., & Cohen, M. X. (2014). Fronto-parietal network oscillations reveal
468 relationship between working memory capacity and cognitive control. *Frontiers in Human*
469 *Neuroscience*, 8(September), 1–13. <https://doi.org/10.3389/fnhum.2014.00761>

470 Hanslmayr, S., Spitzer, B., & Bäuml, K. H. (2009). Brain oscillations dissociate between
471 semantic and nonsemantic encoding of episodic memories. *Cerebral Cortex*, 19(7), 1631–
472 1640. <https://doi.org/10.1093/cercor/bhn197>

473 Harper, J., Malone, S. M., & Bernat, E. M. (2014). Theta and delta band activity explain N2 and
474 P3 ERP component activity in a go/no-go task. *Clinical Neurophysiology*, 125(1), 124–132.

475 <https://doi.org/10.1016/j.clinph.2013.06.025>

476 Herweg, N. A., Solomon, E. A., & Kahana, M. J. (2020). Theta Oscillations in Human Memory.
477 *Trends in Cognitive Sciences*, 24(3), 208–227. <https://doi.org/10.1016/j.tics.2019.12.006>

478 Jas, M., Engemann, D. A., Bekhti, Y., Raimondo, F., & Gramfort, A. (2017). Autoreject:
479 Automated artifact rejection for MEG and EEG data. *NeuroImage*, 159, 417–429.
480 <https://doi.org/10.1016/j.neuroimage.2017.06.030>

481 Jax, S. A., & Buxbaum, L. J. (2010). Response interference between functional and structural
482 actions linked to the same familiar object. *Cognition*, 115(2), 350–355.
483 <https://doi.org/10.1016/j.cognition.2010.01.004>

484 Jax, S. A., & Buxbaum, L. J. (2013). Response interference between functional and structural
485 object-related actions is increased in patients with ideomotor apraxia. *Journal of*
486 *Neuropsychology*, 7(1), 12–18. <https://doi.org/10.1111/j.1748-6653.2012.02031.x>

487 Jensen, O., & Mazaheri, A. (2010). Shaping functional architecture by oscillatory alpha activity:
488 Gating by inhibition. *Frontiers in Human Neuroscience*, 4(November), 1–8.
489 <https://doi.org/10.3389/fnhum.2010.00186>

490 Kalénine, S., Wamain, Y., Decroix, J., & Coello, Y. (2016). Conflict between object structural
491 and functional affordances in peripersonal space. *Cognition*, 155, 1–7.
492 <https://doi.org/10.1016/j.cognition.2016.06.006>

493 Kayser, J., & Tenke, C. E. (2015a). Issues and considerations for using the scalp surface
494 Laplacian in EEG/ERP research: A tutorial review. *International Journal of*
495 *Psychophysiology*, 97(3), 189–209. <https://doi.org/10.1016/j.ijpsycho.2015.04.012>

496 Kayser, J., & Tenke, C. E. (2015b). On the benefits of using surface Laplacian (current source
497 density) methodology in electrophysiology. *International Journal of Psychophysiology*,

498 97(3), 171–173. <https://doi.org/10.1016/j.ijpsycho.2015.06.001>

499 Klimesch, W., Fellinger, R., & Freunberger, R. (2011). Alpha oscillations and early stages of
500 visual encoding. *Frontiers in Psychology*, 2(MAY), 1–11.
501 <https://doi.org/10.3389/fpsyg.2011.00118>

502 Klimesch, W., Freunberger, R., & Sauseng, P. (2010). Oscillatory mechanisms of process
503 binding in memory. *Neuroscience and Biobehavioral Reviews*, 34(7), 1002–1014.
504 <https://doi.org/10.1016/j.neubiorev.2009.10.004>

505 Klimesch, W., Sauseng, P., & Hanslmayr, S. (2007). EEG alpha oscillations: The inhibition-
506 timing hypothesis. *Brain Research Reviews*, 53(1), 63–88.
507 <https://doi.org/10.1016/j.brainresrev.2006.06.003>

508 Kopell, N. J., Gritton, H. J., Whittington, M. A., & Kramer, M. A. (2014). Beyond the
509 connectome: The dynamome. *Neuron*, 83(6), 1319–1328.
510 <https://doi.org/10.1016/j.neuron.2014.08.016>

511 Kourtis, D., & Vingerhoets, G. (2015). Perceiving objects by their function: An EEG study on
512 feature saliency and prehensile affordances. *Biological Psychology*, 110(August), 138–147.
513 <https://doi.org/10.1016/j.biopsycho.2015.07.017>

514 Lachaux, J. P., Rodriguez, E., Martinerie, J., & Varela, F. J. (1999). Measuring phase synchrony
515 in brain signals. *Human Brain Mapping*, 8(4), 194–208. [https://doi.org/10.1002/\(SICI\)1097-0193\(1999\)8:4<194::AID-HBM4>3.0.CO;2-C](https://doi.org/10.1002/(SICI)1097-0193(1999)8:4<194::AID-HBM4>3.0.CO;2-C)

517 Lindemann, O., Stenneken, P., van Schie, H. T., & Bekkering, H. (2006). Semantic activation in
518 action planning. *Journal of Experimental Psychology. Human Perception and Performance*,
519 32(3), 633–643. <https://doi.org/10.1037/0096-1523.32.3.633>

520 Llanos, C., Rodriguez, M., Rodriguez-Sabate, C., Morales, I., & Sabate, M. (2013). Mu-rhythm

521 changes during the planning of motor and motor imagery actions. *Neuropsychologia*, 51(6),
522 1019–1026. <https://doi.org/10.1016/j.neuropsychologia.2013.02.008>

523 Mizelle, J. C., Kelly, R. L., & Wheaton, L. A. (2013). Ventral encoding of functional
524 affordances: A neural pathway for identifying errors in action. *Brain and Cognition*, 82(3),
525 274–282. <https://doi.org/10.1016/j.bandc.2013.05.002>

526 Muthukumaraswamy, S. D., Johnson, B. W., & McNair, N. A. (2004). Mu rhythm modulation
527 during observation of an object-directed grasp. *Cognitive Brain Research*, 19(2), 195–201.
528 <https://doi.org/10.1016/j.cogbrainres.2003.12.001>

529 Osiurak, F., & Badets, A. (2016). Tool Use and Affordance: Manipulation-Based Versus
530 Reasoning-Based Approaches. *Psychological Review*, 123(2).
531 <https://doi.org/10.1037/rev0000027>

532 Osiurak, F., Rossetti, Y., & Badets, A. (2017). What is an affordance? 40 years later.
533 *Neuroscience & Biobehavioral Reviews*, 77(August 2016), 403–417.
534 <https://doi.org/10.1016/j.neubiorev.2017.04.014>

535 Perrin, F., Pernier, J., Bertrand, O., & Echallier, J. F. (1989). Spherical splines for scalp potential
536 and current density mapping. *Electroencephalography and Clinical Neurophysiology*,
537 72(2), 184–187. [https://doi.org/10.1016/0013-4694\(89\)90180-6](https://doi.org/10.1016/0013-4694(89)90180-6)

538 Pineda, J. A. (2005). The functional significance of mu rhythms: Translating “seeing” and
539 “hearing” into “doing.” *Brain Research Reviews*, 50(1), 57–68.
540 <https://doi.org/10.1016/j.brainresrev.2005.04.005>

541 Proverbio, A. M. (2012). Tool perception suppresses 10-12Hz mu rhythm of EEG over the
542 somatosensory area. *Biological Psychology*, 91(1), 1–7.
543 <https://doi.org/10.1016/j.biopsycho.2012.04.003>

- 544 Reynaud, E., Lesourd, M., Navarro, J., & Osiurak, F. (2016). On the neurocognitive origins of
545 human tool use: A critical review of neuroimaging data. *Neuroscience & Biobehavioral*
546 *Reviews*, *64*, 421–437. <https://doi.org/10.1016/j.neubiorev.2016.03.009>
- 547 Sabate, M., Llanos, C., Enriquez, E., & Rodriguez, M. (2012). Mu rhythm, visual processing and
548 motor control. *Clinical Neurophysiology*, *123*(3), 550–557.
549 <https://doi.org/10.1016/j.clinph.2011.07.034>
- 550 Sakreida, K., Effnert, I., Thill, S., Menz, M. M., Jirak, D., Eickhoff, C. R., ... Binkofski, F.
551 (2016). Affordance processing in segregated parieto-frontal dorsal stream sub-pathways.
552 *Neuroscience and Biobehavioral Reviews*, *69*, 89–112.
553 <https://doi.org/10.1016/j.neubiorev.2016.07.032>
- 554 Tallon-Baudry, C., & Bertrand, O. (1999). Oscillatory gamma activity in humans and its role in
555 object representation. *Trends in Cognitive Sciences*, *3*(4), 151–162.
556 [https://doi.org/10.1016/S1364-6613\(99\)01299-1](https://doi.org/10.1016/S1364-6613(99)01299-1)
- 557 Tenke, C. E., & Kayser, J. (2012). Generator localization by current source density (CSD):
558 Implications of volume conduction and field closure at intracranial and scalp resolutions.
559 *Clinical Neurophysiology*, *123*(12), 2328–2345.
560 <https://doi.org/10.1016/j.clinph.2012.06.005>
- 561 Tettamanti, M., Conca, F., Falini, A., & Perani, D. (2017). Unaware processing of tools in the
562 neural system for object-directed action representation. *The Journal of Neuroscience*,
563 *37*(44), 1061–17. <https://doi.org/10.1523/JNEUROSCI.1061-17.2017>
- 564 Thill, S., Caligiore, D., Borghi, A. M., Ziemke, T., & Baldassarre, G. (2013). Theories and
565 computational models of affordance and mirror systems: An integrative review.
566 *Neuroscience and Biobehavioral Reviews*, *37*(3), 491–521.

567 <https://doi.org/10.1016/j.neubiorev.2013.01.012>

568 Töllner, T., Wang, Y., Makeig, S., Müller, H. J., Jung, T.-P., & Gramann, K. (2017). Two
569 Independent Frontal Midline Theta Oscillations during Conflict Detection and Adaptation in
570 a Simon-Type Manual Reaching Task. *The Journal of Neuroscience*, 37(9), 2504–2515.
571 <https://doi.org/10.1523/JNEUROSCI.1752-16.2017>

572 Vanni, S., Revonsuo, A., & Hari, R. (1997). Modulation of the Parieto-Occipital Alpha Rhythm
573 during Object Detection. *The Journal of Neuroscience*, 17(18), 7141–7147.
574 <https://doi.org/10.1523/JNEUROSCI.17-18-07141.1997>

575 Wamain, Y., Gabrielli, F., & Coello, Y. (2016). EEG mu rhythm in virtual reality reveals that
576 motor coding of visual objects in peripersonal space is task dependent. *Cortex*, 74, 20–30.
577 <https://doi.org/10.1016/j.cortex.2015.10.006>

578 Wamain, Y., Sahai, A., Decroix, J., Coello, Y., & Kalénine, S. (2018). Conflict between gesture
579 representations extinguishes μ rhythm desynchronization during manipulable object
580 perception: an EEG study. *Biological Psychology*, 132(January), 202–211.
581 <https://doi.org/10.1016/j.biopsycho.2017.12.004>

582

583

584 **Figure 1.** (A) Virtual environment perceived by the participants. (B) The two possible stimuli-
585 objects manipulated during the experiment. (C) After viewing a fixation cross, one of the
586 two objects randomly appeared. After a time-interval between 800ms and 1200ms,
587 participants heard a tone (i.e. the go-signal) and had to grasp and move the object as fast as
588 possible. During the training phase of the object function, moving one of the two objects
589 opened the box. During the training phase of the object usage, participants had to perform a
590 novel tool-use to open the box with one of the two objects.

591

592 **Figure 2.** Amplitude of oscillatory activity recorded at electrode CPz during the pre- and post-
593 training phases when learning the object usage (N=20; top) and function (N=21; bottom).
594 The training effect (TE) appears particularly important in the theta-band during the learning
595 of the object usage.

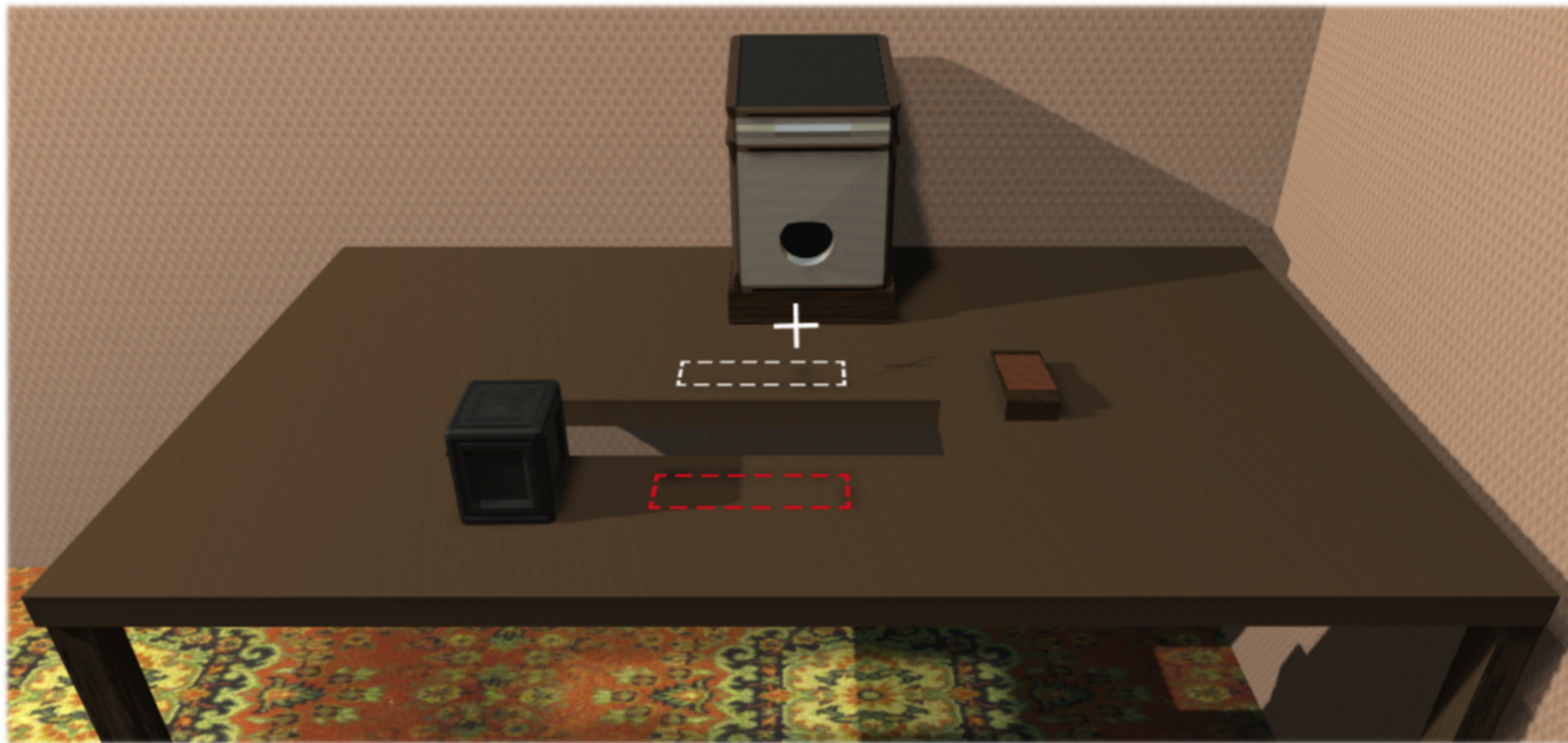
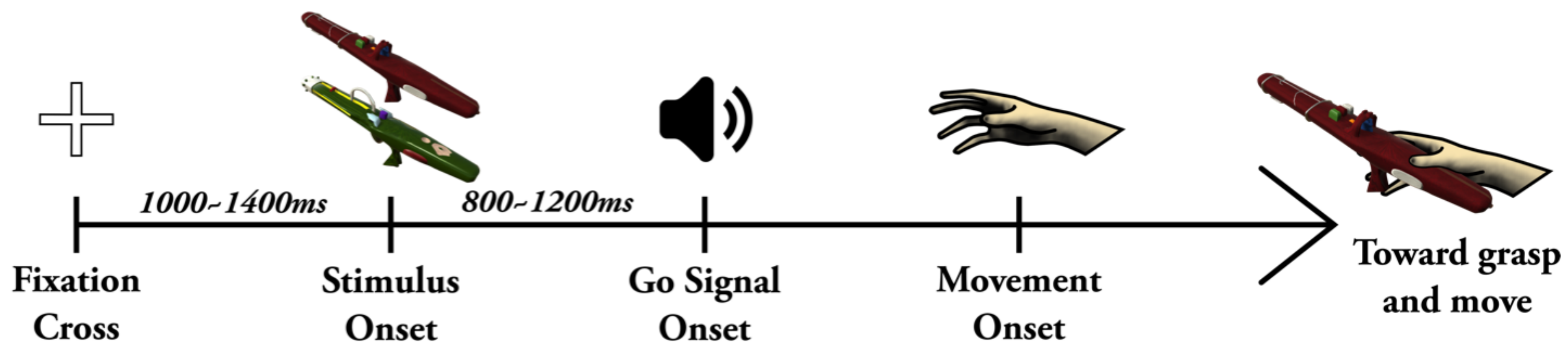
596

597 **Figure 3.** Difference of training effect (TE) between the trained and the non-trained objects on
598 the amplitude of the 8-12 Hz oscillations during visual object processing across scalp (top).
599 Training effects depending on the regions of interest (centro-parietal, occipital, left and right
600 motor areas), the stimulus (trained or non-trained) and the training (learning object usage or
601 function; bottom). Training participants to associate a novel usage and functional
602 knowledge to novel objects prevented the reduction of mu-band amplitude during visual
603 object processing. Error bars represent one standard error of the mean.

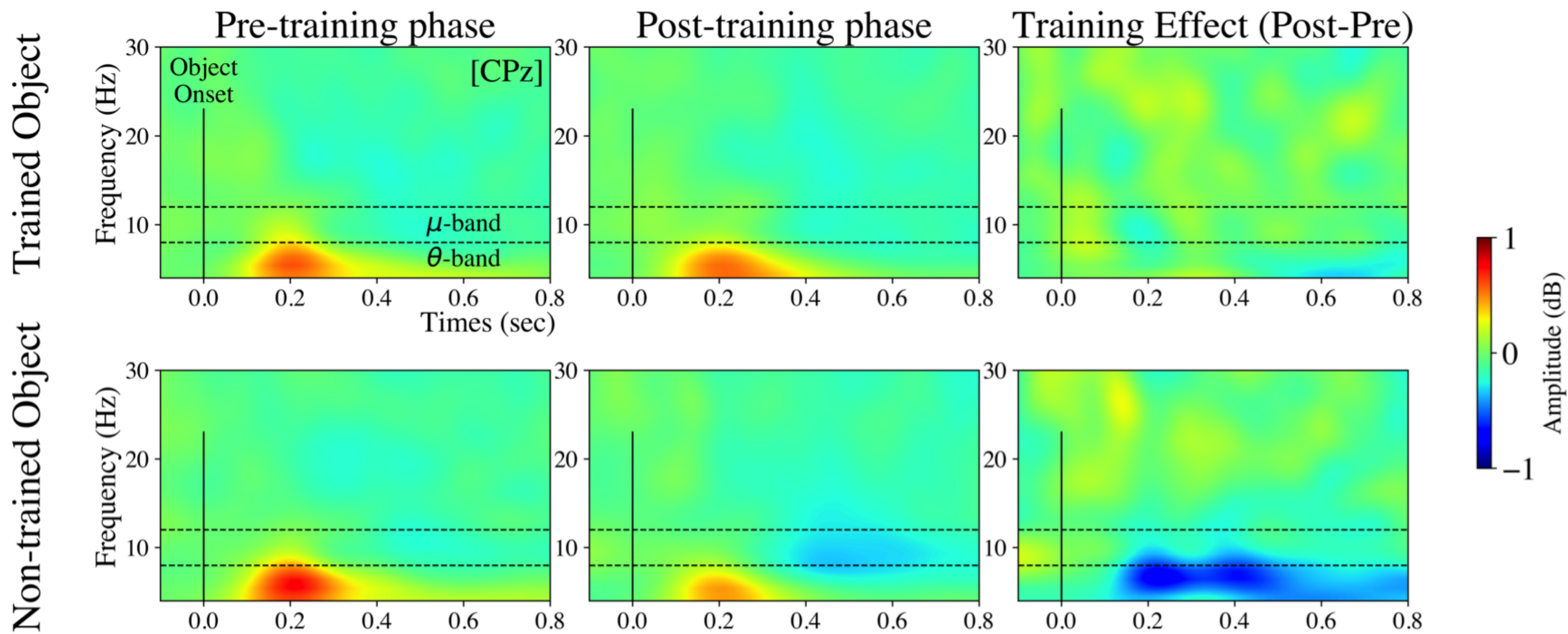
604

605 **Figure 4.** Difference of training effect (TE) between the trained and the non-trained objects on
606 the amplitude of theta-band (4-8 Hz) oscillations during object processing across scalp

607 (top). Training effects depending on the regions of interest (centro-parietal, occipital, left
608 and right motor areas), the stimulus (trained or non-trained) and the training (learning object
609 usage or function; bottom). Learning the usage of a novel object prevented the
610 desynchronization of theta-band oscillations from central to occipital cortical areas during
611 visual object processing. Error bars represent one standard error of the mean.

A**B****C**

Learning Object Usage



Learning Object Function

